Temperature-Dependent Interactions between Photoactivated *Pharaonis* Phoborhodopsin and Its Transducer†

Kentaro Kamada,‡ Yuji Furutani,‡,§ Yuki Sudo,‡ Naoki Kamo,|| and Hideki Kandori*,‡,§

Department of Materials Science and Engineering, Nagoya Institute of Technology, Showa-ku, Nagoya, 466-8555, Japan, Core Research for Evolutional Science and Technology (CREST), Japan Science and Technology Corporation, Kyoto 606-8502, Japan, and Laboratory of Biophysical Chemistry, Graduate School of Pharmaceutical Sciences, Hokkaido University, Sapporo 060-0812, Japan

Received January 10, 2006; Revised Manuscript Received February 25, 2006

ABSTRACT: *Pharaonis* phoborhodopsin (*p*pR, also called *pharaonis* sensory rhodopsin II, *p*sRII) is a receptor for negative phototaxis in *Natronomonas pharaonis*. In membranes, it forms a 2:2 complex with its transducer protein *p*HtrII, and the association is weakened by 2 orders of magnitude in the M intermediate (*p*pR_M). Such a change is believed to correspond to the transfer of the light signal to *p*HtrII. A previous Fourier transform infrared (FTIR) study observed hydrogen-bonding alteration of Asn74 in *p*HtrII in the M state, suggesting a light-signaling pathway from the receptor to the transducer [Furutani, Y., Kamada, K., Sudo, Y., Shimono, K., Kamo, N., and Kandori, H. (2005) *Biochemistry 44*, 2909−2915]. In this paper, we measure temperature dependence of the *p*pR_M minus *p*pR spectra in the absence and presence of *p*HtrII at 250−293 K. Significant temperature dependence was observed for the amide-I vibrations of helices only for the *p*pR/*p*HtrII complex, where the amplitude of amide-I vibrations was reduced at room temperature. ^{13}C-Labeling of *p*pR or *p*HtrII revealed that such spectral changes of helices originate from *p*pR and not *p*HtrII. The hydrogen-bonding alteration of Asn74 in *p*HtrII was temperature-independent, implying that the observed helical structural perturbation in *p*pR takes place in different region. On the other hand, temperature-dependent structural changes of helices were diminished for the complex of *p*pR with the G83C and G83F mutants of *p*HtrII. Gly83 is believed to connect the transmembrane helix and cytosolic linker region in a flexible kink near the membrane surface of *p*HtrII, and its replacement by Cys or Phe abolishes the photosensory function. The present study provides direct experimental evidence that Gly83 plays an important structural role in the activation processes of the *p*pR/*p*HtrII complex. A molecular mechanism of protein structural changes in the *p*pR/*p*HtrII complex is discussed on the basis of the present FTIR results.

Pharaonis phoborhodopsin (*p*pR,[1] also called *pharaonis* sensory rhodopsin II, *p*sRII) is one of the archaeal rhodopsins that have all-*trans*-retinal as a chromophore (*1*−*5*). The retinal forms a Schiff base linkage with Lys205 in the middle of the seventh transmembrane helix (*6*, *7*). *p*pR serves as a photoreceptor in *Natronomonas pharaonis* and forms a signaling complex in archaeal membranes with *pharaonis* halobacterial transducer protein, *p*HtrII (*8*). *p*HtrII is a transmembrane two-helical protein and belongs to a family of transmembrane two-helical methyl-accepting chemotaxis proteins (MCPs) (*9*, *10*). It is well-known that MCPs exist as homodimers composed of 50−60 kDa subunits and form a ternary complex with CheA and CheW. Chemical stimuli activate phosphorylation cascades that modulate flagella motors (*11*−*13*), where MCPs act not only as signal receptors but also as transducers. The light signal is received by *p*pR, a protein different from *p*HtrII, so that specific interactions are required between them (*8*, *14*).

*p*pR transmits light signals to *p*HtrII through the change in such interactions, and *p*HtrII eventually activates phosphorylation cascades that modulate flagella motors. Using this signaling system, haloarchaea avoid harmful near-UV light, displaying what is called a negative phototaxis. *p*pR absorbs maximally at 498 nm, and the light triggers trans−cis photoisomerization of the retinal chromophore in its electronically excited state (*15*), followed by rapid formation of the ground-state species such as the K intermediate (*p*pR_K). Relaxation of *p*pR_K leads to functional processes during the photocycle, where protein structural changes are transmitted from *p*pR to *p*HtrII presumably in the M and/or O states (*16*).

However, what is the molecular mechanism of light-signal transduction in the *p*pR/*p*HtrII complex? Fourier transform

† This work was supported in part by grants from Japanese Ministry of Education, Culture, Sports, Science, and Technology to H.K. and by Research Fellowships from the Japan Society for the Promotion of Science for Young Scientists to Y.F.

* To whom correspondence should be addressed. Telephone and Fax: 81-52-735-5207. E-mail: kandori@nitech.ac.jp.

‡ Nagoya Institute of Technology.

§ CREST.

|| Hokkaido University.

[1] Abbreviations: *p*pR, *pharaonis* phoborhodopsin; *p*HtrII, truncated *pharaonis* halobacterial transducer II expressed from the 1st to 159th position; *p*pR_K, K intermediate of *p*pR; FTIR, Fourier transform infrared; *p*pR_M, M intermediate of *p*pR; DM, *n*-dodecyl-*β*-D-maltoside; PC, L-α-phosphatidylcholine; *p*pR_O, O intermediate of *p*pR; BR, bacteriorhodopsin.

10.1021/bi060047i CCC: $33.50
Published on Web 03/24/2006

infrared (FTIR) spectroscopy is a powerful tool to study detailed structural changes in the activation processes not only for a receptor protein but also for a receptor/transducer complex. In fact, we first applied FTIR spectroscopy to the *p*pR/*p*HtrII complex in 2003 (*17*), finding from spectral analysis of amide-I and amide-A vibrations in the ppR_K minus *p*pR spectra that the complex formation between *p*pR and *p*HtrII perturbs the peptide backbone structure. Hydrogen-bonding network in the Schiff base region was not altered in the *p*pR/*p*HtrII complex. We also observed D_2O-insensitive *p*HtrII-dependent bands at 3479 (−)/3369 (+) cm^{-1} (*17*), which were later assigned to the O−H stretching vibrations of Thr204 (*18*). Last year, we reported difference FTIR spectra between *p*pR and ppR_M, the putative signaling intermediate (*19*). At the ppR_M stage, we observed (i) relaxation of the O−H stretch of Thr204 in *p*pR and (ii) hydrogen-bonding alteration of the C═O group of Asn74 in *p*HtrII and Tyr199 in *p*pR. In addition, amide-I vibrations were surprisingly similar between the samples with and without *p*HtrII. From these results, we concluded that the transducer activation accompanies relaxation of Thr204 in the receptor and hydrogen-bonding alteration of Asn74 in the transducer, during which helices of the transducer perform rigid-body motion without changing their secondary structures (*19*).

These studies revealed the intra- and intermolecular pathways of light-signal transduction, from Lys205 (retinal) of the receptor to Asn74 of the transducer through Thr204 and Tyr199 (*17*−*19*). However, these residues are membrane-embedded, while the importance of protein−protein interactions at the cytoplasmic side is still unclear. In fact, previous spin-labeling studies observed the outward tilt of the F helix in the cytoplasmic region of *p*pR, which forces rotational motion in *p*HtrII (*20*, *21*). In this paper, we measured the ppR_M minus *p*pR spectra in the absence and presence of *p*HtrII in a wide temperature range of 250−293 K. We observed a significant temperature dependence of the amide-I vibrations of helices only for the *p*pR/*p*HtrII complex, where the amplitude of amide-I vibrations was reduced at room temperature. ^{13}C-Labeling of *p*pR or *p*HtrII revealed that such spectral changes originate from *p*pR and not *p*HtrII. Temperature-dependent structural changes of helices were diminished for the complex of *p*pR with the G83C or G83F mutants of *p*HtrII. It is known that replacement of Gly83 of *p*HtrII by cysteine or phenylalanine abolishes the photosensory function (*22*, *23*). Therefore, the importance of the structural role of Gly83 during the signal relay from *p*pR to *p*HtrII is confirmed. The molecular mechanism of protein structural changes in the *p*pR/*p*HtrII complex is discussed on the basis of the present FTIR results.

MATERIALS AND METHODS

Hydrated films of *p*pR or the *p*pR/*p*HtrII mixture were prepared as described previously (*17*, *24*, *25*). *p*HtrII was truncated at position 159. Uniformly ^{13}C-labeled *p*pR or *p*HtrII was prepared by growing cells in a standard minimal medium containing 2 g/L of ^{13}C-D-glucose (Isotec, Inc.) (*17*). The G83C and G83F mutant genes were constructed by PCR using the QuickChange site-directed mutagenesis method. As a template, t-HtrHis was used (*26*). All constructed plasmids were analyzed using an automated sequencer. The *p*pR and *p*HtrII proteins possessing a C-terminal histidine tag were expressed in *Escherichia coli*, solubilized with 1.0% *n*-dodecyl-β-D-maltoside (DM) and purified on a Ni^{2+} column. For the complex, purified *p*pR and *p*HtrII proteins were mixed in 1:1 molar ratio and incubated for 1 h at 4 °C. The samples (*p*pR or the *p*pR/*p*HtrII mixture) were then reconstituted into L-α-phosphatidylcholine (PC) liposomes (*p*pR/PC = 1:50 molar ratio) by removing DM with Bio-Beads (SM-2, Bio-Rad). The PC liposomes were washed 3 times with a buffer at pH 7.0 (2 mM phosphate), and 90 μL of the sample was dried on a BaF_2 window with a diameter of 18 mm.

FTIR spectroscopy was performed as described previously (*19*, *27*, *28*). After hydration by H_2O, the sample was placed in a cell, which was mounted in an Oxford DN-1704 cryostat placed into the Bio-Rad FTS-60 spectrometer. Samples were illuminated with >480 nm light (VY-50, Toshiba) from a 1 kW halogen-tungsten lamp for 2 min, which converted *p*pR to ppR_M. At 273 and 293 K, difference spectra were obtained by subtracting the spectra taken before the illumination from the ones taken during the illumination as described earlier (*28*). The difference spectrum was calculated from the spectra constructed from 128 interferograms. A total of 24 spectra obtained in this way were averaged for the ppR_M minus *p*pR spectrum. At 250 K, the difference spectrum was calculated from the spectra constructed from 128 interferograms recorded after the illumination, subtracting those recorded before the illumination (*19*). We confirmed that identical spectra were obtained by subtracting the spectra taken before the illumination from the ones taken during the illumination as described earlier (*19*). For the comparison of the ppR_M minus *p*pR spectra, we normalized the negative band at 1202 cm^{-1}.

To ensure the reproducibility, we measured the FTIR spectra from two independent preparations (different expressions). In each preparation, two or three films were made and spectra were compared. All of these samples produced the same results.

RESULTS

Temperature-Dependent Helical Structural Changes in the ppR/pHtrII Complex. Figure 1 shows the ppR_M minus *p*pR difference spectra in the absence (a) and presence (b) of *p*HtrII at 250−293 K. In the absence of *p*HtrII, the difference spectra were almost identical to each other, which reproduced the previous observations (*28*). The bands at 1664 (−)/1643 (+) cm^{-1} are the largest in the amide-I region, indicating a structural perturbation of a helix (Figure 1a). Such structural changes take place for the M state regardless of the temperature between 250 and 293 K.

In contrast, a significant temperature dependence was observed for the *p*pR/*p*HtrII complex. Figure 1b shows the ppR_M minus *p*pR difference spectra in the presence of *p*HtrII, where clear spectral variation was seen between different temperatures. In particular, the amide-I vibrations at 1664 (−)/1643 (+) cm^{-1} are significantly reduced at higher temperatures, although the peak positions are not changed. At 250 K, the amplitude of the bands at 1664 (−)/1643 (+) cm^{-1} is slightly smaller for the *p*pR/*p*HtrII complex than for *p*pR (79% in amplitude). On the other hand, the amplitude of the bands for the *p*pR/*p*HtrII complex is less than half of that for *p*pR at 293 K. Such temperature dependence was

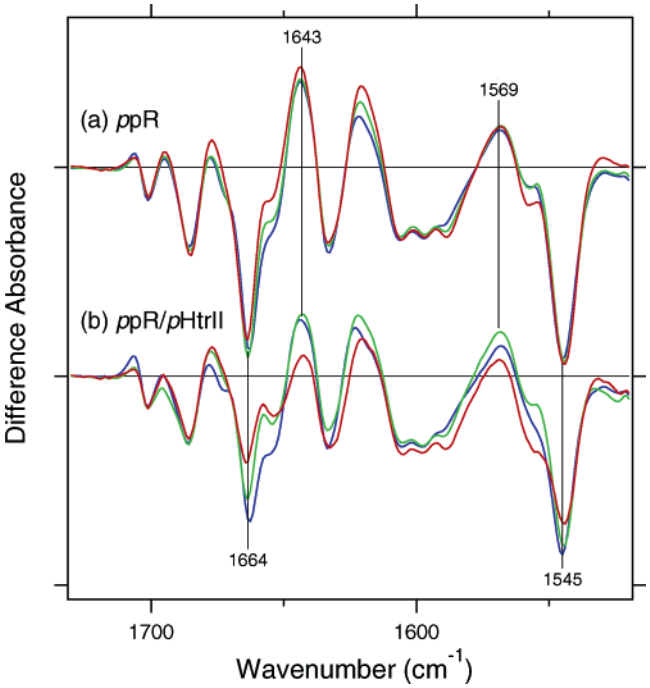

FIGURE 1: ppR$_M$ minus ppR infrared difference spectra in the 1730−1520 cm^{-1} region taken without (a) and with (b) pHtrII. Spectra are measured at 250 K (blue), 273 K (green), and 293 K (red) upon hydration with H_2O. One division of the y axis corresponds to 0.01 absorbance units.

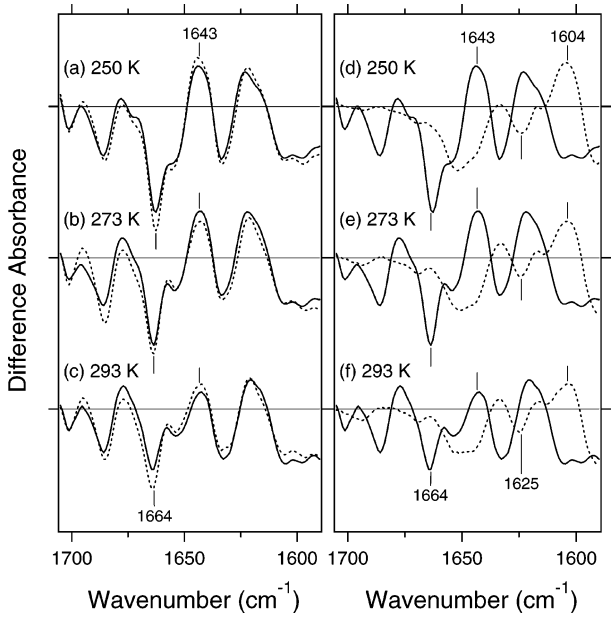

FIGURE 2: ppR$_M$ minus ppR infrared difference spectra for the unlabeled ppR with unlabeled (— of left) and ^{13}C-labeled (··· of left) pHtrII and for the unlabeled (— of right) and ^{13}C-labeled (··· of right) ppR with unlabeled pHtrII in the 1705−1590 cm^{-1} region. Spectra are measured at 250 K (a and d), 273 K (b and e), and 293 K (c and f) upon hydration with H_2O. One division of the y axis corresponds to 0.01 absorbance units.

also reported by the previous time-resolved FTIR study (*29*). A reduction of the bands at 1569 (+)/1545 (−) cm^{-1} at room temperature probably originates from the amide-II vibrations (Figure 1b), which also show structural perturbation of helices. It should be noted that Figure 1 does not contain other spectral components such as from the O intermediate, because the ppR$_O$-characteristic band at 1538 (+) cm^{-1} (*30*) is missing from the spectra in parts a and b of Figure 1. Fingerprint vibrations at 1300−1100 cm^{-1} are identical between 250 and 293 K spectra (data not shown).

This raises an interesting question of the origin of the temperature dependence exclusive for the complex. One possibility is that the amide-I bands of ppR (Figure 1a) are influenced by complex formation with pHtrII. Alternatively, even when similar amide-I bands of ppR are preserved in the complex, additional peptide backbone alterations of pHtrII may result in the reduction of the total amide-I bands. To resolve this, we examined the origin of the bands by use of ^{13}C-labeled samples. Figure 2 compares the ppR$_M$ minus ppR difference spectra of the unlabeled ppR/pHtrII complex (—) with ^{13}C-labeled pHtrII (··· in a−c) or ppR (··· in d−f). Essentially, the same spectra for ^{12}C- and ^{13}C-pHtrII (parts a−c of Figure 2) strongly suggest that the temperature-dependent spectral changes originate from ppR and not pHtrII, because of the minor isotope effect. Spectral deviations at 1695−1685 cm^{-1} in parts a−c of Figure 2 come from the C═O stretching vibration of Asn74 of pHtrII (*19*), which is analyzed in detail below.

Solid and dotted lines are different in parts d−f of Figure 2, indicating that most spectral changes originate from ppR. The bands at 1664 (−)/1643 (+) cm^{-1} for the unlabeled complex (—) shift to lower frequencies, presumably to 1625 (−)/1604 (+) cm^{-1} (···). The intensity of the bands at 1625 (−)/1604 (+) cm^{-1} (··· in parts d−f of Figure 2) is reduced at 293 K in a manner similar to the unlabeled complex (Figure 1b). We thus conclude that all amide-I vibrations in the ppR/pHtrII complex originate from ppR, and the spectral contribution of secondary structural changes in pHtrII itself is minor. This implies that the protein motions of ppR, particularly at the helices, are somehow perturbed by the presence of pHtrII. Such events take place at room temperature but are suppressed at low temperatures such as 250 K. Because the water is frozen at 250 K, the interaction between ppR and pHtrII may be inhibited at such a low temperature.

Temperature-Dependent Secondary Structural Changes of a Helix in the ppR/pHtrII Complex Are Diminished for the Gly83 Mutants of pHtrII. A mechanism by which the secondary structural changes of helices in ppR are perturbed by the presence of pHtrII is interesting and requires further explanation. Yang et al. reported that the replacement of Gly83 in pHtrII by cysteine or phenylalanine diminishes the photosensory function, indicating the important role of Gly83 in the protein structural changes of the ppR/pHtrII complex upon activation (*22*). We thereby studied FTIR difference spectra of the mutants of Gly83. Figure 3 compares the ppR$_M$ minus ppR difference spectra in the ppR/pHtrII complex for the wild-type (a), G83C (b), and G83F (c) pHtrII. It is clear that there is no temperature dependence of amide-I vibrations for G83C and G83F. It should be noted that this observation does not originate from the absence of the interaction between ppR and the mutant pHtrII. They form a complex in the dark as can be argued from the two following facts. First, the decay kinetics of the M state is delayed in the presence of the G83C and G83F mutant pHtrII similar to the wild type (data not shown) (*19*, *31*). Second, the complex-dependent infrared signal of Asn74 of pHtrII is also observed for these mutants (see below). Thus, the G83C and G83F mutant pHtrII forms a complex with ppR resembling the wild-type pHtrII.

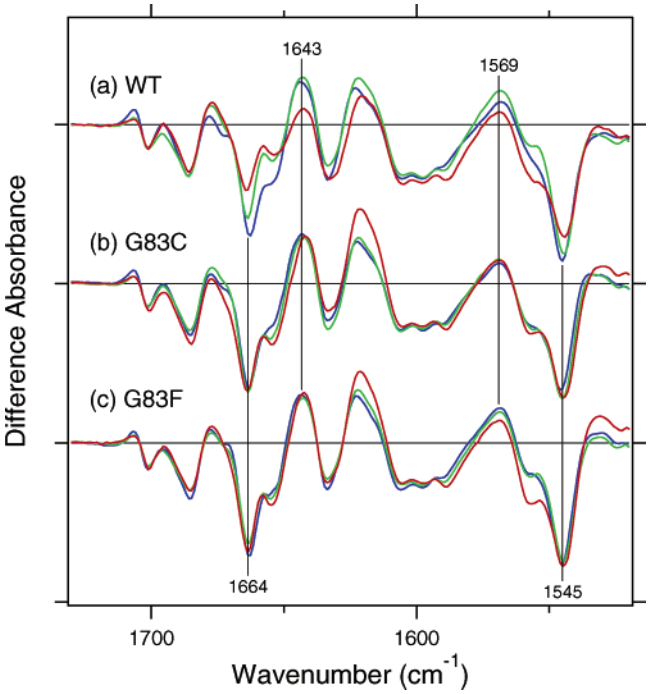

FIGURE 3: *p*ppR$_M$ minus *p*pR infrared difference spectra in the 1730−1520 cm^{-1} region taken with the wild-type (a), G83C (b), and G83F (c) *p*HtrII. Spectra are measured at 250 K (blue), 273 K (green), and 293 K (red) upon hydration with H_2O. One division of the *y* axis corresponds to 0.01 absorbance units.

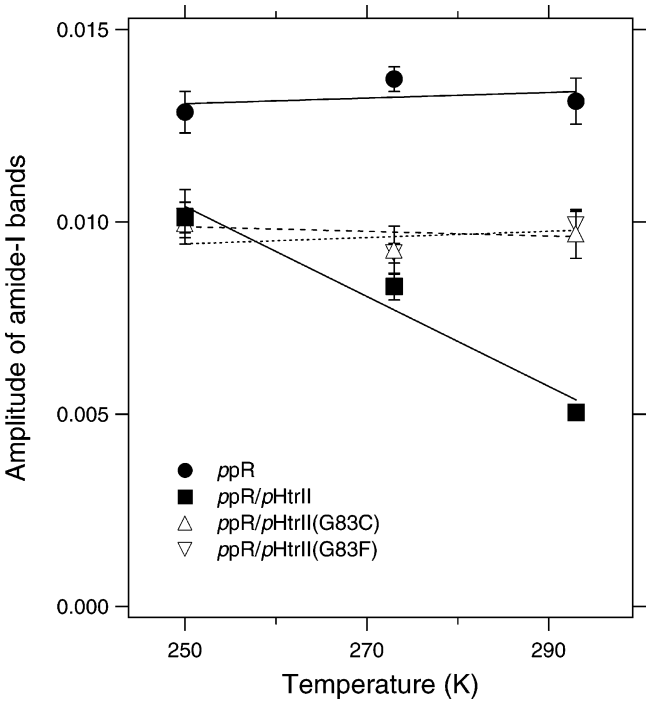

FIGURE 4: Temperature dependence of the amplitude of amide-I vibrations of helices. The absorbance difference between 1643 and 1664 cm^{-1} is plotted versus the temperature, where the spectra are normalized by the negative band at 1202 cm^{-1}. Three independent measurements from different hydrated films were averaged.

Temperature dependence of amide-I vibrations of helices is more clearly seen in Figure 4, where difference in absorbance between 1643 and 1664 cm^{-1} is plotted versus temperature. As shown in Figure 1a, there is no temperature dependence in the absence of *p*HtrII (● in Figure 4), where the difference is 0.013 absorbance units. In contrast, the

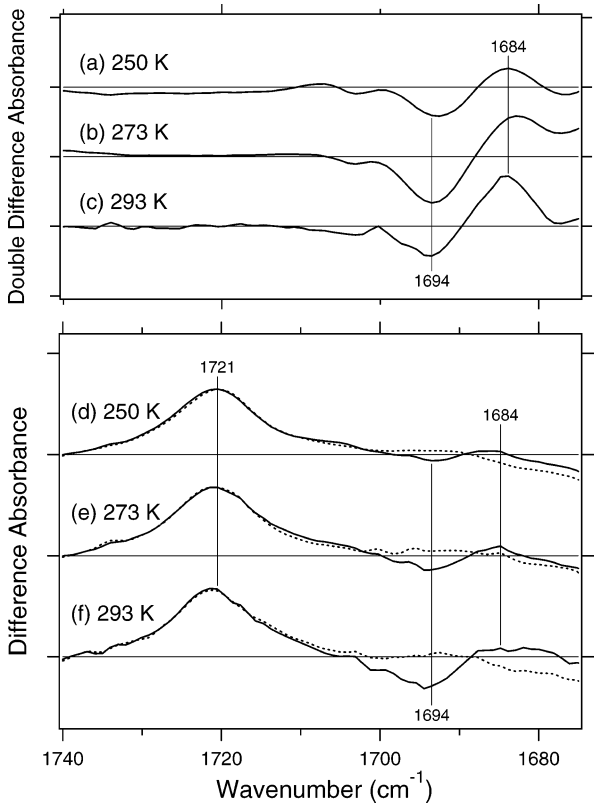

FIGURE 5: (a−c) Double-difference spectra obtained from the data of parts a and b of Figure 1 in the 1740−1675 cm^{-1} region, where the spectra in Figure 1a was subtracted from those in Figure 1b at the corresponding temperatures. Spectra are measured at 250 K (a), 273 K (b), and 293 K (c) upon hydration with H_2O. One division of the *y* axis corresponds to 0.002 absorbance units. (d−f) *p*ppR$_M$ minus *p*pR infrared difference spectra for the ^{13}C-labeled *p*pR without (···) and with (—) unlabeled *p*HtrII in the 1740−1675 cm^{-1} region. Spectra are measured at 250 K (d), 273 K (e), and 293 K (f) upon hydration with H_2O. One division of the *y* axis corresponds to 0.0025 absorbance units.

amplitude of amide-I vibrations is reduced at high temperatures in the presence of the wild-type *p*HtrII (■ in Figure 4). Amplitude of the amide-I bands exhibits an approximately linear correlation with temperature. Such temperature dependence is diminished in the presence of the G83C and G83F mutant *p*HtrII (△ in Figure 4). The difference is 0.010 absorbance units for all of the complexes at 250 K, being considerably smaller than in the absence of *p*HtrII. While the value is not changed for the G83C and G83F mutant *p*HtrII, it decreases about 2-fold for the wild-type *p*HtrII at 293 K. These results strongly suggest that Gly83 of *p*HtrII plays a key role in the helical structural changes of *p*pR.

Hydrogen-Bonding Interaction of Asn74 of the Transducer Is Temperature-Independent and Not Influenced by the Mutation of Gly83. In the previous paper, we revealed that the M formation is accompanied by a hydrogen-bonding alteration of Asn74 in *p*HtrII by identifying its C═O stretching vibrations (*19*). In view of the marked temperature dependence of the amide bands, it is instructive to look at the temperature dependence of the Asn74 bands. Figure 5a represents a double-difference spectrum between the blue spectra in parts a and b of Figure 1, where the spectrum without *p*HtrII (a) is subtracted from that with *p*HtrII (b). The bands at 1694 (−)/1684 (+) cm^{-1} were previously assigned to the C═O stretch of Asn74 by use of ^{13}C-labeling

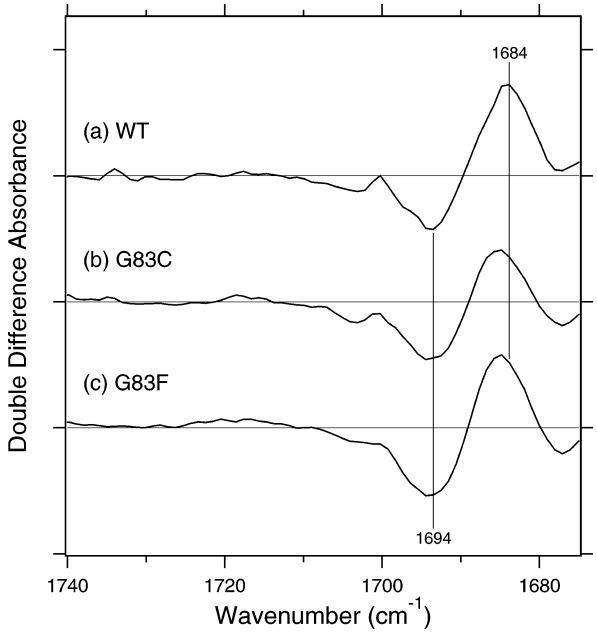

FIGURE 6: Influence of Gly83 mutations on the hydrogen bond of Asn74 in *p*HtrII. Double-difference spectra were obtained between *p*pR$_M$ minus *p*pR spectra at 293 K taken in the presence and absence of *p*HtrII. a is reproduced from Figure 5c for the wild-type *p*HtrII, while b and c are obtained for the G83C and G83F mutant proteins of *p*HtrII, respectively. One division of the *y* axis corresponds to 0.002 absorbance units.

and the N74T mutation (*19*). Parts b and c of Figure 5 represent double-difference spectra between green and red spectra in Figure 1, respectively. The appearance of the 1694 (−)/1684 (+) cm^{-1} bands strongly suggests that the hydrogen-bonding alteration of Asn74 in *p*HtrII also takes place at 273 and 293 K.

The hydrogen-bonding alteration of Asn74 was further examined by use of ^{13}C-labeling. Parts d−f of Figure 5 show the *p*pR$_M$ minus *p*pR infrared difference spectra for the ^{13}C-labeled *p*pR without (···) and with (—) unlabeled *p*HtrII. Using the ^{13}C-labeling of *p*pR but not *p*HtrII, the vibrations in the 1700−1680 cm^{-1} region such as the C═O stretch of Asn105 [1707 (+)/1701 (−) cm^{-1}] (*27*) and the negative 1686 cm^{-1} band of *p*pR can be downshifted by 30−50 cm^{-1}. As a result, the vibration bands because of *p*HtrII will appear more clearly and make the double-difference spectra unnecessary. This was indeed the case. In parts d−f of Figure 5, the ^{13}C═O stretches of Asp75 appear at 1721 cm^{-1}, being shifted from 1765 cm^{-1}. The 1721 cm^{-1} band was not affected by the presence of *p*HtrII and was temperature-independent. In contrast, the bands at 1694 (−)/1684 (+) cm^{-1} were only observable in the presence of *p*HtrII (— in d−f) regardless of the temperature. Thus, we concluded that the 1694 (−)/1684 (+) cm^{-1} bands of Asn74 are not influenced by temperature between 250 and 293 K, suggesting that the hydrogen-bonding alteration of Asn74 observed at 250 K (*19*) persists at room temperature.

Then, we examined the effect of the mutation at Gly83 on the hydrogen bond of Asn74 in *p*HtrII. Figure 6 shows the double-difference spectra between the *p*pR$_M$ minus *p*pR spectra at 293 K, taken in the presence and the absence of *p*HtrII. Similar to the wild-type *p*HtrII (a), the bands at 1694 (−)/1684 (+) cm^{-1} were observed for the G83C (b) and G83F (c) mutant *p*HtrII. This fact indicates that mutations of Gly83 do not affect the hydrogen-bonding alteration of Asn74 upon formation of the M state, although the signal transduction is impaired.

DISCUSSION

In the previous paper, we reported that the *p*pR$_M$ minus *p*pR difference spectra at 250 K are surprisingly similar with and without the transducer protein (*19*). The result strongly suggested that secondary-structure alterations do not occur for *p*HtrII during the activation processes. On the other hand, we found that the hydrogen bond of Thr204 in *p*pR, being altered in the primary K intermediate (*17*, *18*), is restored, while the hydrogen bond of Asn74 in *p*HtrII is strengthened in *p*pR$_M$, presumably because of the change in the interaction with Tyr199 of *p*pR (*19*). These facts provided a light-signaling pathway from Lys205 of the receptor to Asn74 of the transducer through Thr204 and Tyr199. The present work has extended these studies by obtaining the accurate *p*pR$_M$ minus *p*pR difference spectra in a wide temperature range of 250−293 K, providing new insights into the signal transduction mechanism.

In the absence of *p*HtrII, the *p*pR$_M$ minus *p*pR difference spectra were temperature-independent at 250−293 K, which reproduced the previous results (*28*). The largest peak pair in the amide-I region was observed at 1664 (−)/1643 (+) cm^{-1}, indicating structural perturbation of the α helix (Figure 1a). A previous spin-labeling study of *p*pR observed an outward tilt of the F helix in the cytoplasmic region (*20*, *21*), which also takes place in the light-driven proton-pump protein bacteriorhodopsin (BR) (*32*). Thus, the opening of a cleft near the F helix is presumably common for *p*pR and BR. In fact, it is known that *p*pR pumps protons in the absence of *p*HtrII, even though the efficiency is lower than that in BR (*33*). Temperature-independent *p*pR$_M$ minus *p*pR difference spectra suggest that such a cleft opening takes place in a wide temperature range of 250−293 K, although the lack of the BR$_N$-like amide-I changes for *p*pR (*28*, *34*) may suggest a smaller helical motion in *p*pR than in BR.[2]

In contrast to *p*pR, a significant temperature dependence was observed for the *p*pR/*p*HtrII complex, which is clearly illustrated in Figures 1b and 4. The amplitude of amide-I vibrations of helices at 1664 (−)/1643 (+) cm^{-1} was significantly reduced at room temperature. ^{13}C-Labeling of *p*pR or *p*HtrII revealed that such spectral changes originate from *p*pR and not *p*HtrII (Figure 2). The hydrogen-bonding alteration of Asn74 in *p*HtrII was temperature-independent (Figure 5), implying that the observed helical structural perturbation in *p*pR takes place in a different region. On the other hand, temperature-dependent structural changes of helices were abolished for the complex of *p*pR with the G83C and G83F mutants of *p*HtrII (Figure 3). We discuss the molecular mechanism of protein structural changes in the *p*pR/*p*HtrII complex by use of a schematic drawing of the structure (Figure 7).

[2] It should be noted that the origin of the helical structural alteration in the amide-I vibration is not identified even for BR (*34*). Although the F-helix opening occurs at the cytoplasmic surface, the amide-I band can be localized at a different site. Peptide backbone alteration in the membrane may control the rigid-body motion of the F helix, leading to the opening. Much less has been understood for *p*pR$_M$. Therefore, we have to be careful about the structural interpretation, whereas the reported results on *p*pR and BR strongly suggest that the amide bands at 1664 (−)/1643 (+) cm^{-1} originate from the helix F opening.

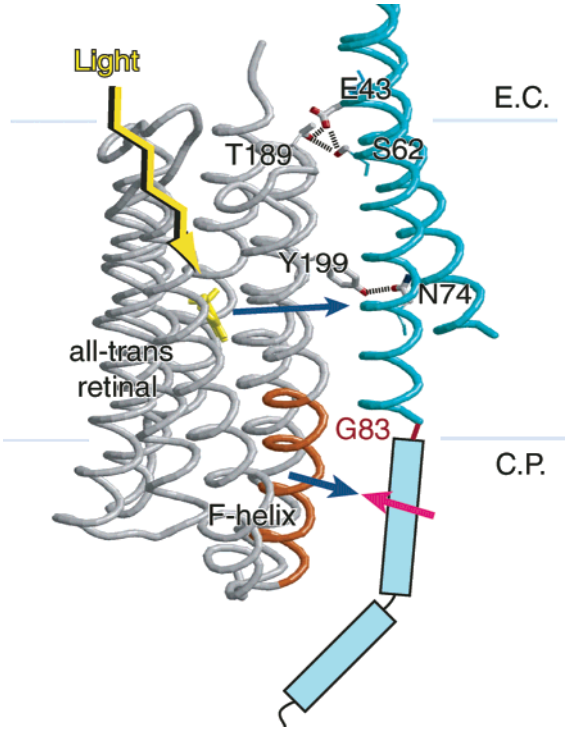

FIGURE 7: Schematic drawing of the signal relay from the receptor (*p*pR) to the transducer (*p*HtrII) in the archaeal photosensory transduction. In the X-ray crystallographic structure of the complex between *p*pR (left) and *p*HtrII (right) (PDB code 1H2S) (*8*), the structure of *p*HtrII at position 83−114 was not determined, suggesting multiple conformations of the region. The association between *p*pR and *p*HtrII originates mostly from van der Waals contacts in the transmembrane region, whereas Tyr199 and Thr189 of *p*pR form hydrogen bonds with Asn74 and Glu43/Ser62 of *p*HtrII, respectively.

Gordeliy et al. crystallized *p*pR complexed with truncated *p*HtrII (residues 1−114), but the structure of the C-terminal half of *p*HtrII (position 83−114) was not determined, presumably because of structural lability (*8*). The residues 83−114 are probably located not in the membrane but in the cytosolic aqueous environment, which may cause structural variations even in a crystal. According to the structure, there are two hydrogen-bonding networks in the transmembrane region of the *p*pR/*p*HtrII complex: one between Tyr199 (*p*pR) and Asn74 (*p*HtrII) and the other between Thr189 (*p*pR) and Glu43/Ser62 (*p*HtrII) (Figure 7). In addition, the interaction of the E−F loop of *p*pR and the cytosolic domain of *p*HtrII has been suggested (*23*, *35*, *36*). These interactions contribute to the strong association of the *p*pR/*p*HtrII complex in the dark [$K_d \sim 160$ nM (*35*, *37*)].

Then, the light-induced protein structural changes lower the K_d value by 2 orders of magnitude in ppR$_M$ [$K_d \sim 15$ μM (*31*)]. This weakened interaction strongly correlates with the ability for the light-signal transduction. However, what is the origin of the changes in the interaction? Previous FTIR studies revealed the changes in the hydrogen-bonding interaction between Tyr199 of *p*pR and Asn74 of *p*HtrII (*19*, *38*). Additional structural changes have been reported at the cytoplasmic surface of the *p*pR/*p*HtrII complex. A spin-labeling study observed the outward tilt of the F helix in *p*pR, which then forces rotational motion of TM2 in *p*HtrII (*20*, *21*, *36*). The experiments using FRET and cross-linking suggested that the accessibility of the helix F of *p*pR and the linker region of *p*HtrII decreases upon illumination and that a mutation at position 83 affects the interaction of these regions (*23*). Gly83 presumably functions as a helix breaker together with Gly84, which disconnects transmembrane helix (TM2) from the helical linker region (Figure 7). Structural flexibility at position 83 is important, because the replacement of Gly83 by cysteine or phenylalanine impairs the signal transduction (*22*). Thus, the reduction of the amide-I vibrations of helices at room temperature in the present study can be interpreted in terms of the impairment of the opening of a cleft near the helix F by the linker region of *p*HtrII. It is likely that the F-helix movement in *p*pR does not or only partially occurs in the *p*pR/*p*HtrII complex, which is manifested as the reduced amide-I vibrations. Such a difference must be correlated with the changed permeability of small reagents into the protein interior (*39*−*41*). It should be noted that, when the structural changes of *p*pR are suppressed by the presence of *p*HtrII, no additional changes were observed for the amide-I bands in *p*HtrII (parts a−c of Figure 2). These facts suggest that the signal transduction from the receptor (*p*pR) to the transducer (*p*HtrII) does not accompany secondary structural alteration of the transducer.

Interestingly, such impairment of the movement of the helix F of *p*pR in the *p*pR/*p*HtrII complex does not occur (i) at 250 K or (ii) for the Gly83 mutants of *p*HtrII. Apparently, the opening of a cleft near the helix F takes place in both cases. In the latter case, a disconnection of the two helices at Gly83 may be lost, so that TM2 is extended beyond position 83. As a consequence, proper interaction changes do not occur in the cytoplasmic region and the movement of the helix F takes place. Similar FTIR spectra were obtained for the wild type at 250 K, whereas the hydrogen-bonding alteration of Asn74 in *p*HtrII was temperature-independent. Therefore, we infer that the structure of the wild-type *p*HtrII at 250 K becomes like that of the Gly83 mutant, and the opening of a cleft near the helix F takes place in *p*pR. In this regard, a key issue may be that the linker region is exposed to an aqueous phase, where freezing of water affects the mobility significantly between 250 and 293 K. If it is the case, a straight line between 250 and 293 K in Figure 4 does not describe the temperature dependence properly. Further studies will reveal a more detailed mechanism on the signal transduction in the complex.

Figure 7 illustrates two signal transduction pathways from *p*pR to *p*HtrII, which may operate by changing the interaction in the complex.[3] One is from retinal/Lys205 of *p*pR to Asn74 of *p*HtrII through Thr204 and Tyr199 in the transmembrane region (blue arrow in Figure 7), which was investigated in the previous FTIR studies (*17*−*19*, *38*). In addition, the opening of a cleft near the helix F through intramolecular structural changes in *p*pR (blue arrow in Figure 7) is perturbed by the linker region of *p*HtrII (red arrow in Figure 7). Such interaction changes are crucial for light-signal transduction, and structural flexibility at position 83 must be important. The mutation at this position and low temperature (250 K) impair the proper interaction changes,

[3] It may be possible that the complex formation with *p*HtrII changes the structure of *p*pR more like ppR$_M$ in the unphotolyzed state, leading to the reduced amide-I bands (Figure 1b). However, X-ray crystallographic studies reported that the structure of *p*pR in the complex is very similar to that of *p*pR in the absence of *p*HtrII (*8*) but different from that of ppR$_M$ in the complex (*42*).

allowing the F-helix movement of *p*pR, and hence, the light-signal transduction is lost.

ACKNOWLEDGMENT

We thank Dr. Kazumi Shimono for valuable discussion.

REFERENCES

1. Kamo, N., Shimono, K., Iwamoto, M., and Sudo, Y. (2001) Photochemistry and photoinduced proton-transfer by *pharaonis* phoborhodopsin, *Biochemistry 66*, 1277−1282.
2. Spudich, J. L., and Luecke, H. (2002) Sensory rhodopsin II: Functional insights from structure, *Curr. Opin. Struct. Biol. 12*, 540−546.
3. Pebay-Peyroula, E., Royant, A., Landau, E. M., and Navarro, J. (2002) Structural basis for sensory rhodopsin function, *Biochim. Biophys. Acta 1565*, 196−205.
4. Sudo, Y., Kandori, H., and Kamo, N. (2004) Molecular mechanism of protein−protein interaction of *pharaonis* phoborhodopsin/transducer and photo-signal transfer reaction by the complex, *Recent Res. Dev. Biophys. 3*, 1−16.
5. Klare, J. P., Gordeliy, V. I., Labahn, J., Büldt, G., Steinhoff, H. J., and Engelhard, M. (2004) The archaeal sensory rhodopsin II/transducer complex: A model for transmembrane signal transfer, *FEBS Lett. 564*, 219−224.
6. Luecke, H., Schobert, B., Lanyi, J. K., Spudich, E. N., and Spudich, J. L. (2001) Crystal structure of sensory rhodopsin II at 2.4 Å: Insights into color tuning and transducer interaction, *Science 293*, 1499−1503.
7. Royant, A., Nollert, P., Edman, K., Neutze, R., Landau, E. M., Pebay-Peyroula, E., and Navarro, J. (2001) X-ray structure of sensory rhodopsin II at 2.1-Å resolution, *Proc. Natl. Acad. Sci. U.S.A. 98*, 10131−10136.
8. Gordeliy, V. I., Labahn, J., Moukhametzianov, R., Efremov, R., Granzin, J., Schlesinger, R., Büldt, G., Savopol, T., Scheidig, A. J., Klare, J. P., and Engelhard, M. (2002) Molecular basis of transmembrane signalling by sensory rhodopsin II-transducer complex, *Nature 419*, 484−487.
9. Rudolph, J., Nordmann, B., Storch, K. F., Gruenberg, H., Rodewald, K., and Oesterhelt, D. (1996) A family of halobacterial transducer proteins, *FEMS Microbiol. Lett. 139*, 161−168.
10. Falke, J. J., Bass, R. B., Butler, S. L., Chervitz, S. A., and Danielson, M. A. (1997) The two-component signaling pathway of bacterial chemotaxis: A molecular view of signal transduction by receptors, kinases, and adaptation enzymes, *Annu. Rev. Cell Dev. Biol. 13*, 457−512.
11. Alley, M. R., Maddock, J. R., and Shapiro, L. (1993) Requirement of the carboxyl terminus of a bacterial chemoreceptor for its targeted proteolysis, *Science 259*, 1754−1757.
12. Maddock, J. R., and Shapiro, L. (1993) Polar location of the chemoreceptor complex in the *Escherichia coli* cell, *Science 259*, 1717−1723.
13. Rudolph, J., and Oesterhelt, D. (1996) Deletion analysis of the che operon in the archaeon *Halobacterium salinarium*, *J. Mol. Biol. 258*, 548−554.
14. Zhang, X. N., Zhu, J., and Spudich, J. L. (1999) The specificity of interaction of archaeal transducers with their cognate sensory rhodopsins is determined by their transmembrane helices, *Proc. Natl. Acad. Sci. U.S.A. 96*, 857−862.
15. Kandori, H., Tomioka, H., and Sasabe, H. (2002) Excited-state dynamics of *pharaonis* phoborhodopsin probed by femtosecond fluorescence spectroscopy, *J. Phys. Chem. A 106*, 2091−2095.
16. Yan, B., Takahashi, T., Johnson, R., and Spudich, J. L. (1991) Identification of signaling states of a sensory receptor by modulation of lifetimes of stimulus-induced conformations: The case of sensory rhodopsin II, *Biochemistry 30*, 10686−10692.
17. Furutani, Y., Sudo, Y., Kamo, N., and Kandori, H. (2003) FTIR spectroscopy of the complex between *pharaonis* phoborhodopsin and its transducer protein, *Biochemistry 42*, 4837−4842.
18. Sudo, Y., Furutani, Y., Shimono, K., Kamo, N., and Kandori, H. (2003) Hydrogen bonding alteration of Thr-204 in the complex between *pharaonis* phoborhodopsin and its transducer protein, *Biochemistry 42*, 14166−14172.
19. Furutani, Y., Kamada, K., Sudo, Y., Shimono, K., Kamo, N., and Kandori, H. (2005) Structural changes of the complex between *pharaonis* phoborhodopsin and its cognate transducer upon formation of the M photointermediate, *Biochemistry 44*, 2909−2915.
20. Wegener, A. A., Chizhov, I., Engelhard, M., and Steinhoff, H. J. (2000) Time-resolved detection of transient movement of helix F in spin-labelled *pharaonis* sensory rhodopsin II, *J. Mol. Biol. 301*, 881−891.
21. Wegener, A. A., Klare, J. P., Engelhard, M., and Steinhoff, H. J. (2001) Structural insights into the early steps of receptor-transducer signal transfer in archaeal phototaxis, *EMBO J. 20*, 5312−5319.
22. Yang, C. S., and Spudich, J. L. (2001) Light-induced structural changes occur in the transmembrane helices of the *Natronobacterium pharaonis* HtrII transducer, *Biochemistry 40*, 14207−14214.
23. Yang, C. S., Sineshchekov, O., Spudich, E. N., and Spudich, J. L. (2004) The cytoplasmic membrane-proximal domain of the HtrII transducer interacts with the E−F loop of photoactivated *Natronomonas pharaonis* sensory rhodopsin II, *J. Biol. Chem. 279*, 42970−42976.
24. Kandori, H., Shimono, K., Sudo, Y., Iwamoto, M., Shichida, Y., and Kamo, N. (2001) Structural changes of *pharaonis* phoborhodopsin upon photoisomerization of the retinal chromophore: Infrared spectral comparison with bacteriorhodopsin, *Biochemistry 40*, 9238−9246.
25. Kandori, H., Furutani, Y., Shimono, K., Shichida, Y., and Kamo, N. (2001) Internal water molecules of *pharaonis* phoborhodopsin studied by low-temperature infrared spectroscopy, *Biochemistry 40*, 15693−15698.
26. Sudo, Y., Yamabi, M., Iwamoto, M., Shimono, K., and Kamo, N. (2003) Interaction of *Natronobacterium pharaonis* phoborhodopsin (sensory rhodopsin II) with its cognate transducer probed by increase in the thermal stability, *Photochem. Photobiol. 78*, 511−516.
27. Kandori, H., Shimono, K., Shichida, Y., and Kamo, N. (2002) Interaction of Asn105 with the retinal chromophore during photoisomerization of *pharaonis* phoborhodopsin, *Biochemistry 41*, 4554−4559.
28. Furutani, Y., Iwamoto, M., Shimono, K., Kamo, N., and Kandori, H. (2002) FTIR spectroscopy of the M photointermediate in *pharaonis* phoborhodopsin, *Biophys. J. 83*, 3482−3489.
29. Bergo, V., Spudich, E. N., Spudich, J. L., and Rothschild, K. J. (2003) Conformational changes detected in a sensory rhodopsin II-transducer complex, *J. Biol. Chem. 278*, 36556−36562.
30. Furutani, Y., Iwamoto, M., Shimono, K., Wada, A., Ito, M., Kamo, N., and Kandori, H. (2004) FTIR spectroscopy of the O photointermediate in *pharaonis* phoborhodopsin, *Biochemistry 43*, 5204−5212.
31. Sudo, Y., Iwamoto, M., Shimono, K., and Kamo, N. (2001) *Pharaonis* phoborhodopsin binds to its cognate truncated tranducer even in the presence of a detergent with a 1:1 stoichiometry, *Photochem. Photobiol. 74*, 489−494.
32. Steinhoff, H., Savitsky, A., Wegener, C., Pfeiffer, M., Plato, M., and Mobius, K. (2000) High-field EPR studies of the structure and conformational changes of site-directed spin labeled bacteriorhodopsin, *Biochim. Biophys. Acta 1457*, 253−262.
33. Sudo, Y., Iwamoto, M., Shimono, K., Sumi, M., and Kamo, N. (2001) Photo-induced proton transport of *pharaonis* phoborhodopsin (sensory rhodopsin II) is ceased by association with the transducer, *Biophys. J. 80*, 916−922.
34. Kandori, H. (1998) Polarized FTIR spectroscopy distinguishes peptide backbone changes in the M and N photointermediates of bacteriorhodopsin, *J. Am. Chem. Soc. 120*, 4546−4547.
35. Sudo, Y., Okuda, H., Yamabi, M., Fukuzaki, Y., Mishima, M., Kamo, N., and Kojima, C. (2005) Linker region of a halobacterial transducer protein interacts directly with its sensor retinal protein, *Biochemistry* 44, 6144−6152.
36. Bordignon, E., Klare, J. P., Doebber, M., Wegener, A. A., Martell, S., Engelhard, M., and Steinhoff, H.-J. (2005) Structural analysis of a HAMP domain: The linker region of the phototranducer in complex with sensory rhodopsin II, *J. Biol. Chem. 280*, 38767−38775.
37. Hippler-Mreyen, S., Klare, J. P., Wegener, A. A., Seidel, R., Herrmann, C., Schmies, G., Nagel, G., Bamberg, E., and Engelhard, M. (2003) Probing the sensory rhodopsin II binding domain of its cognate transducer by calorimetry and electrophysiology, *J. Mol. Biol. 330*, 1203−1213.
38. Bergo, V. B., Spudich, E. N., Rothschild, K. J., and Spudich, J. L. (2005) Photoactivation perturbs the membrane-embedded contacts between sensory rhodopsin II and its transducer, *J. Biol. Chem. 280*, 28365−28369.

39. Sudo, Y., Iwamoto, M., Shimono, K., and Kamo, N. (2002) Association of *pharaonis* phoborhodopsin with its cognate tranducer decreases the photo-dependent reactivity by water-soluble reagents of azide and hydroxylamine, *Biochim. Biophys. Acta 1558*, 63−69.

40. Yoshida, H., Sudo, Y., Shimono, K., Iwamoto, M., and Kamo, N. (2004) Transient movement of helix F revealed by photo-induced inactivation by reaction of a bulky SH-reagent to cysteine-introduced *pharaonis* phoborhodopsin (sensory rhodopsin II), *Photochem. Photobiol. Sci. 3*, 537−542.

41. Zadok, U., Klare, J. P., Engelhard, M., and Sheves, M. (2005) The hydroxylamine reaction of sensory rhodopsin II: Light-induced conformational alterations with C13═C14 nonisomerizable pigment, *Biophys. J. 89*, 2610−2617.

42. Moukhametzianov, R., Klare, J. P., Efremov, R., Baeken, C., Göppner, A., Labahn, J., Engelhard, M., Büldt, G., and Gordeliy, V. I. (2006) Development of the signal in senory rhodopsin and its tranfer to the cognate transducer, *Nature*, Feb. 1 (Epub ahead of print).

BI060047I